International Journal of Advanced Engineering and Technology
ISSN: 2456-7655; Impact Factor: RJIF 5.54
Received: 15-04-2019; Accepted: 18-05-2019
www.newengineeringjournal.com
Volume 3; Issue 3; July 2019; Page No. 36-41

Comparison of the microstructural and mechanical characteristics between gas tungsten arc welded and friction stir welded aa6061 aluminum alloy joints

AS Mohamed[1], SS Mohamed[2], AM Gaafer[3]
[1-3] Mechanical Engineering Department, Faculty of Engineering at Shoubra, Benha University, Cairo, Egypt

Abstract
This work involves a comparison between mechanical properties of AA6061-O welded joints using two different welding processes, typically, gas tungsten arc welding (GTAW) and friction stir welding (FSW). GTAW process was performed on Al AA6061-O plates of 6 mm thickness using ER4030 filler metal according to AWS with tungsten electrode (EWth-2) and various arc voltages and welding currents under argon shielding gas. Friction stir (FS) welded joints were produced using several tool rotational and welding speeds. All welded joints were subjected to X-ray radiography tests and defective joints are excluded. Several mechanical tests, typically, microhardness, tensile and impact tests were carried out to evaluate the mechanical performance of the welded joints. The results revealed that AA6061-O FS welded joints exhibit higher mechanical properties than those obtained by GTAW.

Keywords: friction stir welding (FSW), gas tungsten arc welding (GTAW), mechanical properties, microstructure, aluminum alloys

1. Introduction
The welding processes can be classified as fusion welding and solid-state welding processes [1]. In fusion and solid-state welding, heat and pressure are applied either externally or internally to perform welding. In solid-state welding, the heat is applied internally while the pressure is applied externally. The applied pressure generates a heat that can rise the temperature of the base material to a temperature lower than the melting temperature. Usually, in solid-state welding, a filler materials are not applied. Friction welding (FW) and friction stir welding (FSW) are under this category. While in fusion welding, either heat or pressure is required to apply from external source. External filler materials may be or may be not used. All kinds of gas welding processes and arc welding processes such as submerged arc welding (SAW), metal arc welding (GMAW) and gas tungsten arc welding (GTAW) are under this category.
The GTAW or tungsten inert gas (TIG) welding is an arc welding process that uses a non-consumable elctrode made from tungesten to perform welding. During the GTAW process, an inert shielding gas is used to protect the electrode and weld region from oxidation. Normally a filler material is used. The GTAW is used to weld catbon steels, stainless steels and several non-ferrous metals such as aluminum, copper, and magnesium alloys. The GTAW is an easy and inexpensive welding technique that can produce sound and high quality weldements, however, it is slower than most of other welding techniques. The weld quality in GTAW is primarily controlled by many factors such as workpiece characteristics, electrode quality, filler material, power source type, and welder procedure [2, 3].
Friction stir welding (FSW) is a solid-state joining technique that was developed by The Welding Institute (TWI) in 1991 [4]. Nowadays, FSW has a fast development in several industries, in particular, the marine and aerospace industries. In this process, a non-consumable tool, consists usually from a cylinderical shoulder and a threaded pin, is plunged into the weld line untill the shoulder contacts with the surface of the workpiece and then the tool traverses along the weld line. In FSW, the heat is generated mainly due to the friction between the shoulder and the surface of the workpiece. This heat is sufficient to rise the temperature of the welded region to about 0.8 of the melting temperature. FSW can be performed at lower temperatures than the conventional fusion welding processes. This means that the welding defects that may occur due to the solidification of molten metals can be avoided. FSW is commonly used for joining high strength aluminum alloys, which were previously considered as unweldable by fusion welding processes.
It is well known that it is difficult to weld aluminum and its alloys using fusion welding techniques [5]. This is due to the presence of the aluminum oxide film on the surface of the workpiece. This film should be removed from the surfaces before welding. Moreover, several defects such as hot cracks and porosity may takes place during the melting and solidification processes. The choice of the proper filler material, welding proceduers and welding parameters is significant to avoid these defects. Usually, both of GTAW and FSW techniques are used for welding aluminum alloys. Several investigations reported a comparison between the microstructural and mechanical characteristics of FSW and GTAW welded joints [6-11]. For instance, Muñoz *et al.* [6] studied microstructural and mechanical characteristics of TIG and FSW welds of Al–4.5Mg–0.26Sc heat-treatable aluminium alloys. They reported that joints fabricated using FSW technique showed higher mechanical properties than those fabricated using TIG. The yield strengths of FSW and TIG welded joints were reduced by 20% and 50% when compared with base metal. Wang *et al.* [7] studied the the effect of welding processes (FSW and TIG) on the fatigue properties of 5052 aluminum-welded joints. They showed that the fatigue strengths of FS welded joints are better than

those of TIG welded joints. The FSW welded regions exhibited finer grains and narrower heat affected zone (HAZ) than the welded regions of joints welded using TIG technique. Such fine grain structure can assist in hindering the propagation of cracks and result in longer fatigue life. Zhao *et al.* [11] reported that the mechanical properties of Al–Mg–Sc FS welded joints are much better than those of TIG welded joints. The tensile and yield strengths of FSW joint are 19% and 31% higher than those of TIG joints, respectively.

The present investigation is a comparative study of the effect of the welding technique on the microstructure and mechanical characteristics of AA6061-O aluminum alloy welded joints produced using GTAW (TIG) and FSW welding techniques. Moreover, the effect of the process parameters of these techniques on the quality of AA6061-O welded joints was investigated.

2. Experimental procedures

2.1 Base Material

The AA6061-O (Al-Mg-Si) wrought heat-treatable aluminum alloy was used as a base material. The chemical composition of the AA6061 alloy is listed in Table 1. Table 2 lists the mechanical properties for the AA6061-O alloy.The alloy was obtained in the form of large rolled plates having 6 mm thickness. The large plates then were machined into plates with dimensions of 100 mm (width)× 250 mm (length) × 6 mm (thickness).

Table 1: The chemical composition of the AA6061-O aluminum alloy (wt.-%).

Mg	Si	Fe	Ti	Zn	Cr	Cu	Mn	Al
0.9	0.8	0.13	0.1	0.015	0.35	0.27	0.001	Bal.

Table 2: The mechanical properties of the AA6061-O alloy.

Tensile strength (MPa)	Yield strength (MPa)	Elongation (%)	Hardness (HV)
124	60	25	35

2.2 Friction Stir Welding Process

The FSW was carried out using conventional milling machine. A threaded pin tool, with the dimensions shown in Fig. 1, was used to perform the FSW. The tool is made from R18 high speed steel. The FSW was performed using different tool rotational and welding speeds. The tool rotational speeds are 710, 1120 and 1400 rpm while the traverse speeds are 63, 80 and 100 mm/min. The tilte angle and shoulder plunging depth were kept constant at 3º and 0.2 mm, respectively.

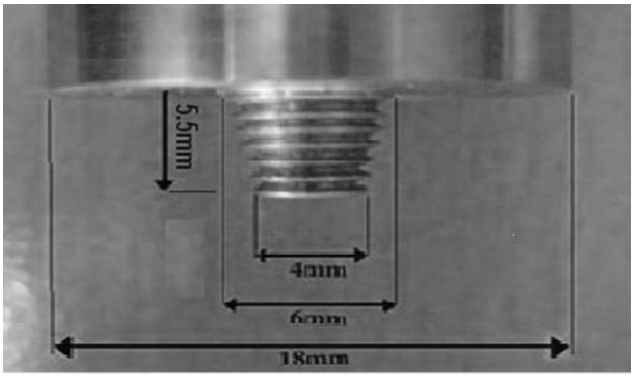

Fig 1: The FSW tool (Dimensions in mm).

2.3 GTAW Process

The edges of the plates to be welded were was machined to have V-groove with an angle of 65º and a root face of 2 mm. Edge preparation of specimen and 'V' butt joint configuration was shown in Figure 2. Befor welding, the groove was cleaned using a wire brush, followed by cleaning with acetone, to remove the oxide layer and dirt or grease adhering to the surface of the plates. The GTAW was carried out using a 2.4 mm ER4030 (AlSi5) filler rod with a chemical composition listed in Table 3. The machine used for GTAW was completely digitised Fronius MagicWave 3000 with AC power source that is used especially for aluminium applications. The GTAW was performed using three different votages of 14, 17, and 19 V, and three different welding currents of 140, 160 and 175 A. An argon (99.97% pure) was used as a shielding gas with a flow rate 10 lit/min. The Tungsten (99.75% pure) electrode has 3.2 mm diameter.

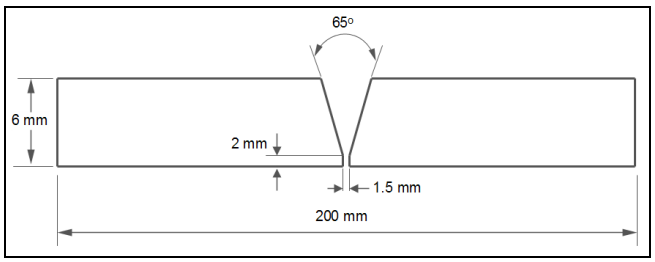

Fig 2: A schematic illustration of the GTAW joints edge preparation.

Table 3: The chemical composition of the ER 4043 filler (wt.-%)

Si	Fe	Cu	Mn	Mg	Cr	Zn	Sn	Al
5.0	0.4	0.1	0.08	0.06	0.25	0.15	0.15	Bal.

2.4 Visual and X-Ray Radiography

The FSW and GTAW joints were subjected to visual examination to detect the possible surface defects. The joints were also subjected to X-ray radiographic analysis to detect the internal defect in weldments such as pores and discontinuities at weld nugget. The X-ray radiographic unit operated at 125 kV, 5 mA for a duration of 1.5 min. After the aforementioned inspections, the joints without defects were approved, while the defective joints were excluded.

2.5 Macro- and Microstructural Investigations

The metallographic samples were cut in a direction perpendicular to the welding direction. The samples were then ground and polished using standard metallographic techniques. After that, the samples were etched by using Keller's reagent. Microstructural analysis was performed using Olympus optical microscope. The grain size measurements were carried out using line-intercept technique via metallurgical image analyzer.

2.6 Mechanical Tests

The Vickers micro-hardness measurements were taken on the cross-sections perpendicular to the welding direction using a load of 50 gf and a dwell period of 10 s. The microhardness distribution of the welded regions was determined.Tensile tests were carried out on room temperature using a Wolpert universal testing machine according to ASTM E-8M with a cross head speed of 5 mm/min. Tensile specimens were machined from the

welded specimens from the transverse direction with a gauge length of 25 mm and width of 9 mm. The ultimate tensile strength (UTS) of the welded joints was identified. Weld centerline Charpy V-notch tests were conducted to evaluate the impact behavior of the welded joints. The standard sub-size Charpy notched specimens were machined from the welded joints. From each welding condition, a minimum of three tensile and impacts tests were carried and the average value is determined. The fracture surfaces of the failed tensile and impact specimens were examined using scanning electron microscope (SEM).

3. Results and discussion

3.1 Visual and X-Ray Radiography

Figure 3 shows a typical general apperance as well as the x-ray radiography of a joint FS welded using 1400 rpm and 100 mm/min. The FS welded joints exhibited lateral flash in most of the welds (see Fig. 3a). This is resulting from the outflow of the plasticized material from the beneath of the shoulder which expels large volumes of material in the form of surface flash. Semi-circular tracks on the surface of the FS welded joints is clearly seen. These tracks resulted from the shoulder of the welding tool [12]. Surface cracks or unbonded zones were not observed on the surfaces of FS welded joints. The keyhole defect, at the end of joints, which caused by the welding tool are observed. The x-ray radiography image shown in Fig. 3b indicated that the joints are free from internal defects such as tunnel defects and cavities. These observation indicates that the heat energy produced during FSW is optimum which resulted in a FSW joints. Lower rotational speeds and/or higher travel speeds may be insufficient to produce the required amount of frictional heat and an incomplete material stirring may occur at welding zone. Figure 4 shows a typical general apperance as well as the x-ray radiography of a joint welded GTAW technique using 140 A and 19 V. Visual examinations showed that the weld is clean and there are no welding defects such as lack of fusion and surface breaking pores. The x-ray image shown in Fig. 4b shows that there are no internal defects were observed in the GMAW joints.

Fig 3: Photographs shows (a) general appearance and (b) X-Ray Radiography of joints FS welded using 1400 rpm and 100 mm/min.

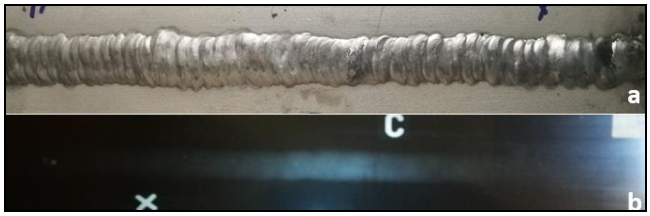

Fig 4: Photographs shows (a) general appearance and (b) X-Ray Radiography of joints welded by GTAW technique using 140 A and 19 V.

3.2 Macro- and Microstructural Characteristics of the Welded Joints

Sample macrographs of the macrostructures of joints welded using FSW and GTAW techniques in Figure 5. As indicated by the x-ray radiographic examinations, that there are no internal defects in the joints welded using FSW abd GTAW techniques indicating the suitable selection of the welding processes parameters for both techniques. Figure 5a indicates the different regions that the FS welded joints are mainly consists of. These regions are the base material, (BM) heat affected zone (HAZ), thermo-mechanically affected zone (TMAZ), and stirred or nugget zone (SZ). Figure 5b shows that, beside the base material, the structure of the GTAW joints consists of, the heat affected zone (HAZ), in which a recrystallization process was occured, and the fusion zone (FZ) with a typical solidifcation process structure.

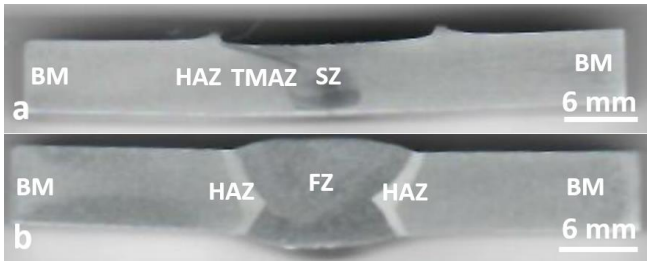

Fig 5: Macrographs of the joints welded using; (a) FSW at 1120 rpm and 100 mm/min; and (b) GTAW at 175 A and 17 V.

Figure 6 shows typical microstructures of base material, stirred zone of a FS welded joint and the fusion zone of a GTAW joint. The microstructure of the base metal consists of large elongated α-Al grains which is a typical of rolled structure (see Fig. 6a). The FSW stirred zone consists of very fine α-Al grains. The FZ has a microstructure of a typical cast structure with larger grain size. Both macro- and micro segregation are observed in all the welded regions. In GTAW samples, the HAZ grains showed an unrecrystallized elongated shape. While in FSW samples, the microstructure of the HAZ was similar to the base alloy.

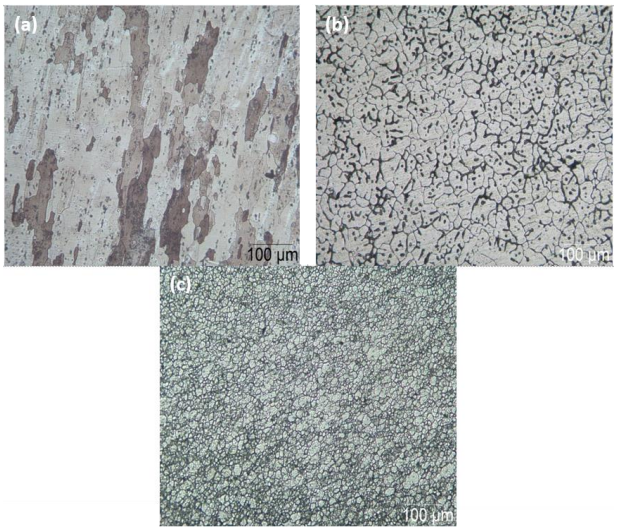

Fig 6: Optical micrographs for typical microstructures of (a) BM, (b) FZ of GTAW welded joint (175 A, 14 V) and (c) SZ of FS welded joint (1120 rpm, 80 mm/min).

Variation of the average size, at the center of the welded zone, of the primary α-Al grains with the different FSW and GTAW process parameters is illustrated in Fig. 7. Generally, the FS welded joints exhibited lower grain size at the center of SZ when compared with those joints produced using GTAW.

In GTAW, the electric arc is used to provide thermal energy to melt the workpiece and the filler materials. After solidification of molten pool metal, a coarsen ingot grain structure is produced. While, in the FSW, the material undergoes intense plastic deformation at elevated temperature (without melting), resulting in the formation of fine grain structure [9]. For FSW joints, increasing the welding speed and/or tool rotational speed show had a slight influence on the average grain size in the stirred zone. Within the range of the investigated FSW process parameters, the average sizes of the grains at the SZ were found to be vary between 10 to 15 µm. For GTAW, increasing the welding current and/or reducing the welding voltages slightly increase(s) the average size of the primary α-Al grain at the centers of the fusion zones. The minimum and maximum average grain sizes were about 20 µm and 30 µm, respectively. These values were observed at the center of the fusion zone of joints welded using 140 A and 17 V and 160 A and 14 V, respectively.

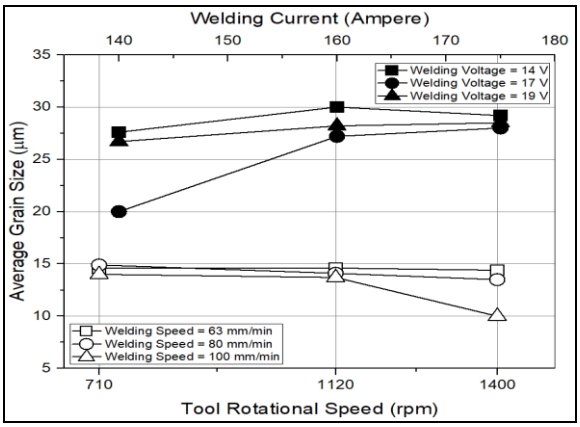

Fig 7: Variation of the average size, at the center of the welded zone, of the primary α-Al grains with the different FSW and GTAW process parameters.

3.3 Microhardness of FSW and GTAW Joints

The AA6061-O base metal showed an average hardness value of about 35 HVN. Figure 8 shows the microhardness profiles of the cross-sections of FSW and GTAW joints produced using different process parameters. The microhardness of welded regions was higher than the base metal, but the microhardness of the FS weld joints was about 15% higher than GTAW weld joints. The GTAW weld joints showed the highest average microhardness of 68 HVN at weld center. The FS welded joints showed highest average microhardness of about 80 HVN at the weld center. The results revealed that increasing the tool rotational speed and/or the welding speed slightly increase(s) microhardness at FS welded regions. For example, at constant welding speed of 63 mm/min, increaseing the tool rotational speed from 710 to 1400 rpm increased the microhardness at the center of the SZ from 72 to 80 VHN. The HAZ and TMAZ exhibited higher microhardness values when compared with the BM.

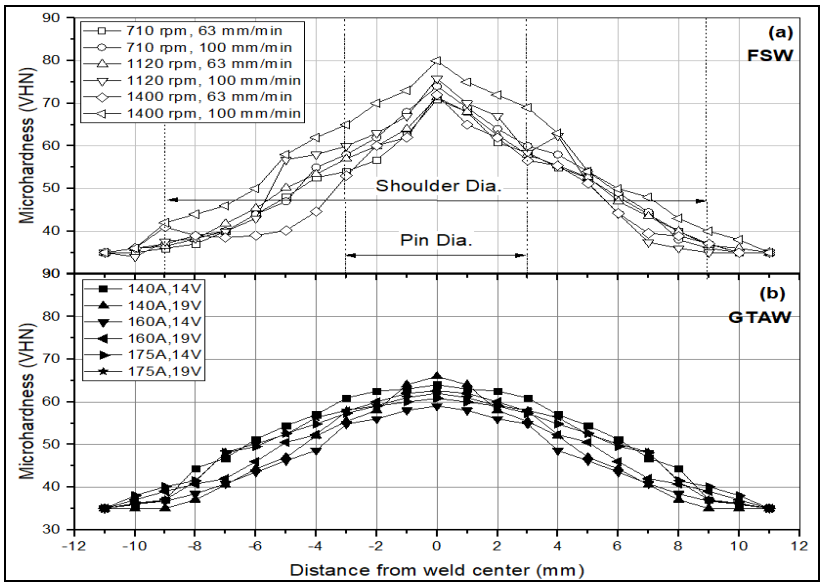

Fig 8: The microhardness profiles of the cross-sections of joints welded using: (a) FSW and (b) GTAW at different welding process parameters.

The increase of the hardness of the FS welded regions when compared with those welded using GTAW may attribute to the the finer microstructure in the FS welds. The finer grain structure the better mechanical properties. In case of GTAW welding, very high temperature increases the peak temperature of the molten weld pool causing slow cooling rate, in turn causes relatively coarser grain structure in the fusion zone as observed from the micrographs shown in Fig. 6b. These microstructures generally offer lower resistance to indentation.

3.4 Tensile Strength of FSW and GTAW welded Joints

The tensile strengths of the FSW and GTAW specimens are listed in Tables 4 and 5, respectively. The FSW specimens exhibited higher tensile strengths and joint efficiencies when compared with the GTAW specimens. The maximum tensile strength was 145 MPa for specimens FS welded using 1400 rpm and 100 mm/min. While the maximum tensile strength was 128 MPa for GTAW specimens using 140 A and 17 V. Increasing the tool rotational speed or increasing the welding speed increases the tensile strength of FS welded joints. While increasing the welding current form 140 A to 175A reduced the tensile strength of GTAW welded joints. It has been found that increasing the welding voltage from 14V to 17V has no practical influence of the tensile strength of GTAW joints.

Table 4: The Tensile strength of FS welded specimens.

Specimen	Tool rotational speed (rpm)	Welding speed (mm/min)	Tensile Strength, UTS (MPa)
1	710	63	126
2		80	120
3		100	134
4	1120	63	129
5		80	133
6		100	137
7	1400	63	130
8		80	139
9		100	145

Table 5: The Tensile strength of GTAW specimens.

Specimen	Current (Ampere)	Voltage (Volts)	Tensile Strength, UTS (MPa)
1	140	14	118
2		17	128
3		19	122
4	160	14	106
5		17	120
6		19	112
7	175	14	110
8		17	100
9		19	115

The fracture surfaces of the failed tensile specimens as observed under the SEM are displayed in Figure 9. The fractured surfaces of both FSW and GTAW failed tensile specimens consists of dimples, which indicates that a ductile fracture mechanism under the action of tensile loading was occurred. An appreciable difference exists in the size and shape of the dimples with respect to welding processes.

Coarse dimples were observed at the fractured surfaces of GTAW joints (see Fig. 9b), while fine dimples were observed at the fractured surfaces of FSW joints (see Fig. 9a).

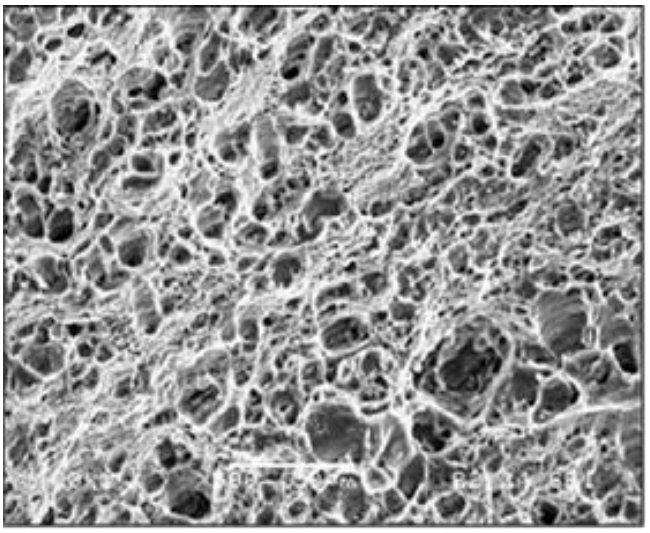

(a)

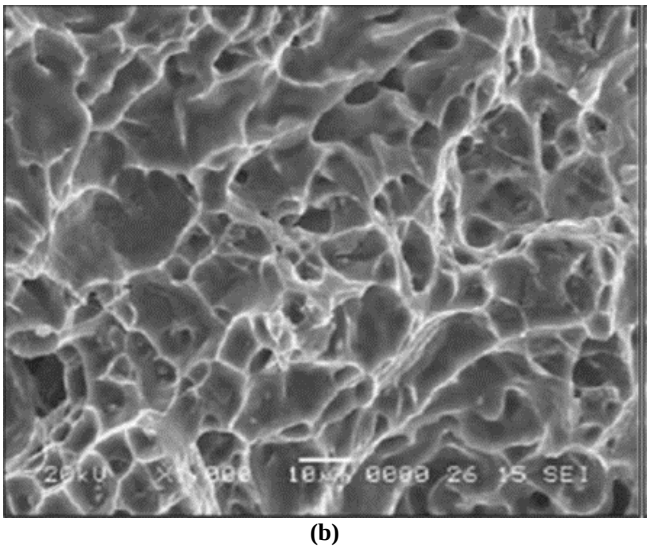

(b)

Fig 9: SEM micrograph of typical fracture surfaces of (a) FSW and (b) GTAW tensile specimens.

3.5 Impact Strength of FSW and GTAW Joints

The impact strengths of the FSW and GTAW specimens are listed in Tables 6 and 7, respectively. The results revealed that the FSW joints exhibited signficantly higher impact strengths when compared with the GTAW joints as well as the AA6061-O base alloy. The impact strength of the base alloy was about 17 J. The maximum impact strength was about 25 J for specimens FS welded using 710 rpm and 63 mm/min. There is no relation between the impact strength and the tool rotational and welding speeds has been observed. The GTAW specimens exhibited significantly lower impact strengths than the base alloy. The maximum impact strength was about 8 J for specimen GTAW using 175A and 19 V.

Table 6: Impact strength of FSW specimens.

Specimen	Tool rotational speed (rpm)	Welding speed (mm/min)	Impact toughness (J)
1	710	63	25
2		80	21
3		100	16
4	1120	63	17
5		80	20
6		100	21
7	1400	63	23
8		80	22
9		100	20

Table 7: Impact strength of FSW specimens.

Specimen	Current (Ampere)	Voltage (volts)	Impact toughness (J)
1	139	14	4
2		17	3
3		19	3
4	160	14	3
5		17	6
6		19	4
7	175	14	5
8		17	3
9		19	8

4. Conclusions

The main results of the current study are as follows

1. The FS welded joints exhibited higher microhardness values when compared with those regions welded using GTAW. For FSW regions, increasing the tool rotational and/or the welding speeds slightly increases the microhardness at the FS welded regions.
2. The joints welded using FSW exhibited better tensile and impact strengths when compared with those welded using GTAW. The FS welded joints showed impact and tensile strengths higher than the AA6061-O base alloy. While the GTAW joints showed signicantly lower impact strength and in most cases tensile strength than the base alloy.
3. Increasing the tool rotational speed and/or welding speed increase(s) the tensile strength, while have no determined influence on the impact strength, of joints welded using FSW.

5. References

1. Handbook ASM. Welding, Brazing, and Soldering, 1993, 6.
2. Sindo Kou. Welding Metallurgy, John Wiley & Sons, 2nd Edition, 2003.
3. Muyiwa Olabode, Paul Kah, Jukka Martikainen. Aluminium alloys welding processes: Challenges, joint types and process selection Proc IMechE Part B: J Engineering Manufacture. 2013; 227(8):1129-1137.
4. Daniela Lohwasser, Zhan Chen. Friction stir welding: From basics to applications, Woodhead Publishing Limited, 2010.
5. Gene Mathers. The welding of aluminium and its alloys, Woodhead Publishing Limited, 2002.
6. CabelloMuñoz A, Rückert G, Huneaua B, Sauvage X, Marya S. Comparison of TIG welded and friction stir welded Al–4.5Mg–0.26Sc alloy, J. of Materials Processing Technology. 2008; 197(1-3):337-343.
7. Xunhong Wang, Kuaishe Wang, Yang Shen, Kai Hu, Comparison of fatigue property between friction stir and TIG welds, J. of University of Science and Technology Beijing. 2008; 15(3):280-284.
8. Guofu Xu, Jian Qian, Dan Xiao, Ying Deng, Liying Lu, Zhimin Yin. Mechanical Properties and Microstructure of TIG and FSW Joints of a New Al-Mg-Mn-Sc-Zr Alloy, Journal of Materials Engineering and Performance. 2016; 25(4):1249-1256.
9. Xuefeng Lei, Ying Deng, Yongyi Peng, Zhimin Yin, Guofu Xu. Microstructure and Properties of TIG/FSW Welded Joints of a New Al-Zn-Mg-Sc-Zr Alloy, Journal of Materials Engineering and Performance. 2013; 22:2723-2729.
10. Morteza Ghaffarpour, Mohammad Kazemi, Mohammad Javad Mohammadi Sefat, Ahmad Aziz, Kamran Dehghani. Evaluation of dissimilar joints properties of 5083-H12 and 6061-T6 aluminum alloys produced by tungsten inert gas and friction stir welding, Proc IMechE Part L: J Materials: Design and Applications. 2017; 231(3):297-308.
11. Juan Zhao, Feng Jiang, Haigen Jian, Kang Wen, Long Jiang, Xiaobo Chen. Comparative invesation of tungsten inert gas and friction stir welding characteristics of Al–Mg–Sc alloy plates Materials and Design. 2010; 31:306-311.
12. Podržaj P, Jerman B, Klobčar D. Welding Defects At Friction Stir Welding, Metalurgija. 2015; 54(2):387-389.